

Published in final edited form as:

Nat Neurosci. 2015 January ; 18(1): 66–74. doi:10.1038/nn.3891.

Retinal output changes qualitatively with every change in ambient illuminance

Alexandra Tikidji-Hamburyan^{#1,4}, Katja Reinhard^{#1}, Hartwig Seitter¹, Anahit Hovhannisyanyan¹, Christopher A. Procyk², Annette E. Allen², Martin Schenk³, Robert J. Lucas², and Thomas A. Münch^{1,§}

¹Retinal Circuits and Optogenetics, Centre for Integrative Neuroscience and Bernstein Center for Computational Neuroscience, University of Tübingen, Germany

²Faculty of Life Science, University of Manchester, Manchester M13 9PT, United Kingdom

³Department for General, Visceral and Transplant Surgery, Institute for Experimental Surgery, University Hospital Tübingen, Germany

⁴Current address: Dept. of Neurosurgery and Hansen Experimental Physics Laboratory, Stanford University, Stanford CA 94305, USA

These authors contributed equally to this work.

Abstract

The collective activity pattern of retinal ganglion cells, the retinal code, underlies higher visual processing. How does the ambient illuminance of the visual scene influence this retinal output? We recorded from isolated mouse and pig retina and from mouse dLGN *in-vivo* at up to seven ambient light levels covering the scotopic to photopic regimes. Across each luminance transition, the majority of ganglion cells exhibited qualitative response changes, while maintaining stable responses within each luminance. Strikingly, we commonly observed the appearance and disappearance of ON responses in OFF cells and vice versa. Such qualitative response changes occurred for a variety of stimuli, including full-field and localized contrast steps, and naturalistic movies. Our results suggest that the retinal code is not fixed but varies with every change of ambient luminance. This finding raises new questions about signal processing within the retina and has intriguing implications for visual processing in higher brain areas.

Introduction

The mammalian visual system functions over a wide range of light intensities, spanning roughly a dozen orders of brightness magnitude. Specialized photoreceptors, namely rods

Users may view, print, copy, and download text and data-mine the content in such documents, for the purposes of academic research, subject always to the full Conditions of use: http://www.nature.com/authors/editorial_policies/license.html#terms

§Correspondence address: thomas.muench@cin.uni-tuebingen.de.

Author contribution: A.T.-H., K.R., and T.A.M. designed the study. MEA recordings and spike sorting were performed by A.T.-H., K.R., H.S. and A.H. and analyzed by A.T.-H., K.R. and T.A.M. Patch-clamp experiments and immunohistochemistry were conducted and analyzed by H.S. and T.A.M. In-vivo experiments were designed by C.A.P., A.E.A. and R.J.L., performed by C.A.P. and A.E.A., and analyzed by C.A.P., A.E.A. and K.R. Pig eyes were provided by M.S. Manuscript was prepared by A.T.-H., K.R. and T.A.M. with the help of H.S., C.A.P., A.E.A. and R.J.L.

and cones, are used to deal specifically with low and high light conditions. At low light intensities, only rods are active (scotopic vision). With increasing luminance, cones become active (mesopic vision), while at high luminance, rods saturate but cones remain active (photopic vision). Already in the outer retina, signals from the photoreceptors are both combined within and distributed across more than ten different bipolar cell types. In the inner retina, the bipolar cell terminals interact with amacrine cell interneurons to bring about sophisticated responses in the output neurons of the retina, the ganglion cells. The diversity of ganglion cells is characterized by physiological parameters¹ as well as by functional specifications such as directional selectivity, approach sensitivity, object motion sensitivity and many more². On a simpler level, all ganglion cells can be classified by their response polarity to step-like changes in brightness: ON cells increase spiking activity to light increments, OFF cells to light decrements, and ON-OFF cells to both. This property is often called “polarity” and is one of the most basic features for further classification of ganglion cells in the vertebrate retina.

It is not well understood how the properties of ganglion cell responses (i.e. the retinal output) vary with changes in ambient luminance. On one hand, it is conceivable that adaptation in retinal circuitry counteracts the changes in ambient luminance, to maintain a stable representation of the incoming visual scene. On the other hand, several reports suggest that the retinal output is altered with changing ambient luminance. Some of these are linked to the switch from scotopic to mesopic vision, i.e. from purely rod mediated to mixed rod-cone mediated signaling. Examples include color vision³, changing responses due to surround activation⁴⁻⁶, changes in temporal and spatial frequency processing^{7, 8}, APB- and strychnine-resistant OFF responses appearing to dim high-contrast stimuli⁹, or luminance-dependent inhibitory modulation of rod signals¹⁰. In addition, the coexistence of several parallel rod pathways¹¹ might allow for different retinal processing within the scotopic range as well, e.g. the primary rod pathway shifts from encoding of single photons to encoding of contrast modulations¹². Furthermore, light adaptation switching from circuit-based to photoreceptor-based mechanisms has been found within both scotopic¹³ and photopic regimes¹⁴. Finally, melanopsin-driven changes in retinal responses have been described within the photopic range¹⁵. Most of these reports concentrate on individual building blocks of the retinal circuit, and each describes luminance-dependent changes over a limited range of light intensities. What is missing is a systematic description of the retinal output and its modulation across a wide range of light intensities, from scotopic to photopic light levels.

We asked whether luminance-dependent changes of the responses of ganglion cells are a widespread phenomenon, or if they are restricted to few cell types or specific luminance transitions. Using multi-electrode array recordings from isolated mouse retina, we made a systematic survey of ganglion cell responses across many orders of ambient luminance, in discrete steps separated by one log unit. We found that the output of the retina was qualitatively different at each tested light level. For example, we found OFF cells gaining or losing ON responses, and vice versa. Such response changes occurred to both simple stimuli and complex natural movies. Sometimes, but not always, these changes depended on modifications of the center-surround receptive field structure or on GABA-mediated inhibition. Consequently, diverse mechanisms seem to underlie the response changes in

different ganglion cell types. In addition, we show that such alterations of the retinal output are not restricted to the isolated mouse retina, but can also be observed *in-vivo*, where the changing output of the retina is reflected by changing activity of dLGN neurons, and in the retina of another species, the pig. It thus appears that luminance-dependent changes of retinal output are a phenomenon that is preserved across species, and that higher visual centers are exposed to these changes.

Results

Experimental paradigm

We presented our visual stimuli (gray scale images) to the isolated mouse retina using a digital projector (Supplementary Fig. 1). The ambient light level was set by placing neutral density (ND) filters into the light-path, such that the intensity of the stimulus could be attenuated without changing the computer-controlled images presented by the projector. Consequently, the contrast of the stimuli remained constant during the experiment (Fig. 1a), independent of the ambient light level. The actual physical intensity of the stimuli associated with each ND-filter is shown in Fig. 1b. According to our estimation (see Methods), ND8 and ND7 correspond to scotopic conditions, ND6 weakly activates cones, ND5 is fully mesopic, and ND4 is photopic. Unless otherwise noted, we started our experiments from low intensity (ND8) and increased it in the course of the experiment (i.e., from ND8 to ND4 in 1-log-unit steps). The retina was kept at each ambient luminance for 20 to 70 min, and we showed the same set of stimuli at each light level.

With this experimental paradigm we recorded from ganglion cells using multi-electrode arrays (MEAs) and compared their responses across different ambient light levels, initially using spatially homogeneous contrast steps (“full-field steps”) of positive and negative contrast (“white step” and “black step”, $\pm 66\%$ Weber contrast, Fig. 1a). We will refer to the increases of a cell’s spike rate to light increments as ‘ON’ responses (both after the white step onset and black step termination), and to light decrements as ‘OFF’ responses (both after the black step onset and white step termination).

Luminance-dependent changes of retinal output

To our surprise, the majority of ganglion cells changed their response type (ON, OFF, or ON-OFF) at different ambient luminance. The example cell in Fig. 2a had OFF responses to all light decrements, but its ON responses were not consistent across light levels. First, they were absent at ND8 but present at ND7 to ND4. Second, when present, they occurred with either short or long latency, measured as time-to-peak of the firing rate (labeled in Fig. 2a as “early” and “delayed”, respectively). Third, during any given light level, the ON responses to the two stimuli (white and black steps) were either the same, i.e. they were absent (ND8) or had the same latency (ND4), or they had different latencies (ND7, ND6 and ND5 for the cell in Fig. 2a). We will refer to the latter as “asymmetry” of the response at a given luminance. In summary, the OFF responses of this cell at the different light levels (ND8 to ND4) differed from each other only quantitatively (amplitude, duration, and moderate latency changes), whereas the ON responses were also affected qualitatively.

Under a “qualitative change” of a response across light levels we understand not only its presence/absence, but also alternations between early and delayed responses. Indeed, early and delayed responses, as seen in Fig. 2a, seem to be two distinct response categories, and not merely separate realizations of a continuous latency distribution. The distributions of the response latencies (time-to-peak, Fig. 2b), measured separately in ON cells and OFF cells, and separately for ON and OFF responses, was monomodal for the preferred contrast, i.e. for ON responses in ON cells and for OFF responses in OFF cells (top row), with a median time-to-peak between 130 and 140 ms. In contrast, the distributions of latencies for responses to the anti-preferred contrast (bottom row) have an additional mode peaking between 600 and 800 ms, in both ON cells and OFF cells. In other words, delayed ON responses occurred only in OFF cells, whereas delayed OFF responses occurred only in ON cells. The bimodality of the distribution indicated two categories of responses and let us treat early and delayed responses as qualitatively different. In our analysis below, we concentrated only on the qualitative response changes. Quantitative aspects were not considered.

Importantly, the response patterns of ganglion cells usually remained stable while probed at the same luminance level (tested up to 70 minutes; luminance levels with unreliable responses were excluded from the analysis, see Methods). When the response pattern of a cell changed at luminance transitions, the new pattern was already observed at the first stimulus presentation. The earliest time point we tested was 10 s after the luminance transition because a luminance increase by 1 log unit itself evoked a strong response in all cells.

The cell in Fig. 2a could be classified as “OFF” at some light levels, and as “ON-OFF” at other light levels, based on its full-field step responses. Since such luminance-dependent response changes were common in many ganglion cells, we used an ON/OFF classification based on properties of their linear filters. We calculated the linear filters from responses to Gaussian white noise full-field flicker (see Methods). Cells with a downward deflected linear filter were marked as OFF, and cells with an upward deflected filter as ON. In contrast to full-field step responses, almost all cells had consistent linear filter polarities over all luminance levels. The cell in Fig. 2a fell into the OFF category at each light level, despite its changing ON responses. Note that with such a classification scheme, ON-OFF cells will not be categorized as such, but they would fall into either the ON or OFF category depending on which input was predominant; similarly, cells with an exceptionally strong surround might be mistaken for a cell of opposite polarity. Furthermore, if ON and OFF inputs were very well balanced, the cell would have a noisy linear filter. However, such cases were rare, and we excluded from the analysis all cells with noisy or changing linear filters across light levels (34 out of 517 recorded units were excluded).

We obtained 219 OFF and 264 ON cells (based on their linear filter properties) from 15 wild type retinas. The validity of this ON/OFF classification approach was supported by the observation that > 97.5% of ganglion cells from the ON-group consistently responded to light increments (i.e. their preferred stimulus) at all light levels, and > 97.4% of cells from the OFF-group consistently responded to light decrements. It follows that luminance-dependent changes mostly occurred in response to the anti-preferred contrast. In the

following analysis, we concentrated on the responses to anti-preferred contrast steps, and we describe the ON responses in OFF cells first.

ON responses in OFF ganglion cells

Across all light levels tested, only 9% of our OFF cells never had an ON response. The number of cells displaying early or delayed ON responses changed at different ambient light levels (Fig. 3a). Almost 100% of OFF cells had no ON responses at ND8, whereas at ND5, this number fell below 20%. Interestingly, the early and delayed responses could also co-occur (most often at ND5). They were still easily separable in most cases due to the considerable difference in their latencies (examples for co-occurrence can be seen in Figs. 4,7 and Supplementary Fig. 3).

At every transition of ambient luminance, the ON responses of a considerable fraction of OFF cells changed (Fig. 3b), ranging from 38% at the ND8/ND7 transition (within the scotopic regime) to 83% at the ND6/ND5 and ND5/4 transitions. Overall, 89% of the OFF cells changed their responses at least once between ND8 and ND4. The response changes were diverse. At any given light level, some cells would lose a certain response type, others would gain it, and some cells would not change. Furthermore, the responses to white steps and black steps changed asymmetrically (Fig. 3a). For example, note at ND6 the predominance of delayed responses to the white step and early responses to the black step, and an opposite ratio at ND5.

In summary, the presence of ON responses and their variability across light levels were two prominent features in OFF cells: we found that early and delayed ON responses in OFF cells can appear/disappear with changing ambient light levels, that they can occur independently or together during a response, and that they can differ for white and black contrast steps. These findings suggest that these early and delayed ON responses in OFF cells may have independent origins and be heterogeneously affected in different OFF cell types by the immediate stimulus history (i.e. white or black step) and by ambient luminance.

OFF responses in ON ganglion cells

Occurrences of OFF responses in ON cells (Fig. 3c,d for summary, Fig. 4a,b for examples) were less common than occurrences of ON responses in OFF cells. In fact, most ON cells were strongly suppressed by light decrements such that their spiking activity fell below their spontaneous firing rates, often to zero. Black steps often suppressed spiking for the entire stimulus duration (2 s), and white step termination for about 500 ms (Fig. 4a). Possibly, strong pre- or postsynaptic inhibition counteracted excitation and decreased the occurrence of the OFF responses. Indeed, there were almost no OFF responses to black steps (Fig. 3c), with the exception of ND4 (photopic light level, 11% of ON cells had early OFF responses). Delayed OFF responses were observed quite frequently after white step termination, especially in scotopic and mesopic light levels (ND7 to ND5).

In our experiments, the luminance-dependent qualitative change of response patterns was such a surprising yet prominent feature of the majority of ganglion cells, that this raises concerns about how trustable and stable these observations are. We tested the following: (1) How strongly are the different response types bound to a particular ambient luminance? (2)

Do these response changes occur in morphologically identified ON and OFF cells? (3) Is this finding restricted to the *in-vitro* conditions, or may it also be observed *in-vivo*? (4) How much of the responses variability is due to the ‘unnatural’ stimulus properties of full-field contrast steps? Furthermore, we investigated the contribution of center-surround receptive field interactions, GABAergic inhibition, and rod-cone interactions to the mechanism of qualitative luminance-dependent response changes.

Response patterns are bound to individual light levels

As described above, the response patterns of ganglion cells were stable at each individual light level but could change after a luminance increase. We next tested if ganglion cell responses would revert when the luminance returns to the previous level (see protocol cartoon in Fig. 5a). Indeed, in the ND8 to ND5 luminance ranges, all recorded cells that changed their responses at a luminance transition ($n=16$ from 2 retinas) immediately reverted to the previous pattern after an intermittent exposure to either lower or higher luminance levels (Fig. 5b,c shows the responses of an example neuron). However, once exposed to ND4 (photopic level), cells did not immediately return to the response they had at ND5 earlier. This may be due to stronger bleaching caused by this light level ($\sim 10^4$ $R \cdot \text{rod}^{-1} \text{s}^{-1}$), or due to some light adaptation triggered during that light level which reverses only slowly. In an additional set of experiments discussed below (Supplementary Fig. 3), we found $n = 2/15$ cells that did not revert to their previous response pattern at the ND7 light level after they had a different pattern during an interleaved exposure to ND6, while $n=13/15$ cells reverted to their previous response pattern.

Taken together, these results suggest that specific response patterns of ganglion cells are strongly associated with distinct luminance levels rather than with the history of luminance or with a luminance-independent drift.

Confirmation using single-cell recordings

The majority of cells in our data set had ON-OFF responses at least at one light level. Our cell-type classification based on linear filter polarity cannot identify “classical” ON-OFF cells (i.e. cells stratifying in both ON and OFF sublaminae of the inner plexiform layer, and having short-latency responses to both light increments and decrements) and distinguish them from “real” ON cells or OFF cells (i.e. cells with dendrites stratifying exclusively in the ON or OFF sublamina). To confirm that the latter can indeed have responses to anti-preferred contrast steps at some light level(s), we recorded action potentials from individual ganglion cells using patch electrodes. Most cells were filled with neurobiotin and imaged with confocal microscopy to assess whether they had typical ON or OFF morphology (Fig. 6a–c).

We recorded from three PV-5 ganglion cells, the well-studied^{16, 17} mouse homolog of the transient OFF-alpha cell (monostratified in the OFF sublamina of IPL; $n=2/3$ cells confirmed with the neurobiotin marker). All three cells had delayed ON responses up to ND5 which disappeared at the photopic light level ND4. For one cell, we repeatedly switched between ND4 and ND5, and the responses reliably reverted (Fig. 6d). Consistent with the related MEA experiments (Fig. 5), switching from ND4 back to ND5 did not lead

to an immediate re-appearance of the delayed ON responses; here they re-emerged about 1 minute after the luminance switch. 4 out of 5 additional cells of unknown types, stratifying exclusively in the OFF (n=3) or ON (n=2) sublamina (Fig. 6e), had luminance-dependent response changes, confirming our findings based on MEA recordings.

Luminance-dependent response changes in-vivo

One important caveat of the results described so far is that they have been recorded from the isolated retina, and that these experiments can last several hours. Do luminance-dependent response changes also happen in the *in-vivo* situation? To test this, we recorded from the dorsal lateral geniculate nucleus (dLGN) of anesthetized mice (Fig. 7a) and projected step stimuli into their eyes that were comparable in absolute intensity and contrast to the stimuli we used for the *in-vitro* recordings (Fig. 7b). Consistent with our findings in the *in-vitro* retina preparation, in the dLGN 18 out of 28 units (n=5 mice) changed their responses qualitatively with changing ambient luminance (Fig. 7c). With the *in-vivo* preparation we could also test higher light levels than in the *in-vitro* experiments (ND3 and ND2, see also Discussion). More than one third of the recorded neurons changed their responses also within the photopic regime (ND4/3 and ND3/2), including the example shown in Fig. 7d.

These observations suggest that luminance-dependent qualitative changes of retinal ganglion cell responses also occur *in-vivo*, and that these changes are reflected in the thalamus. This confirms scattered reports of this phenomenon in the literature³.

Luminance-dependent changes to naturalistic movies

Full-field contrast steps are easy to analyze and interpret. However, it is not a natural stimulus for the retina and visual system in general. The retina might employ specific mechanisms to stabilize the output to a more natural stimulus when it is presented under varying luminance conditions. We tested this by stimulating the retina with a naturalistic movie repeatedly shown at different light levels.

Ganglion cells (n=172 units from 8 retinas) responded to the natural movie with interleaved sequences of spike bursts (“events”) and silence, as described previously¹⁸. Such bursting events presumably correspond to features in the movie that are relevant to this ganglion cell. If a cell had a robust bursting event at some light levels but not at others, we classified this as a qualitative response change (see Methods for details).

We observed such qualitative changes in 57% of the units (n=98/172). For each of these units, some features (scenes of the movie) evoked a response at all light levels tested, and other features evoked a response only at certain light levels (Supplementary Fig. 2a,b). Some units (n=55) were also tested with our full-field step stimulus. Response changes to the movie stimulus and to the full-field step stimulus seemed to occur rather independently from each other (Supplementary Fig. 2c). This suggests that ambient luminance can alter different receptive field properties of ganglion cells, some of which are triggered by a homogeneous full-field step, some by a stimulus with more complex temporal and spatial properties.

Cells' periphery involved in only some response changes

Most ganglion cells' receptive fields consist of spatially distinct center and periphery. Stimulation of the center and periphery can evoke responses of opposite polarities in some ganglion cells¹⁹. What is more, it is known that the receptive field structure of some cells changes during light adaptation⁵. Thus, the changing response patterns that we observed in our experiments might have been caused by luminance-dependent changes in the balance of the receptive field center and periphery. To test this, we stimulated the retina with disks of 150 μm diameter with identical contrast properties as the full-field steps (n=107 units in 4 retinas).

We observed the same variety of response types to the localized disk stimulus as for the full-field stimulation. 80% of the units changed the response type to the disk stimulus at least at one luminance transition, while 20% had stable responses at all light levels (Fig. 8a). At any individual luminance transition, between 44% and 61% of the units changed their responses. We also mapped the receptive fields of all units using a binary noise checkerboard flicker stimulus and measured how much of the disk stimulus lies within the receptive field center (Fig. 8b). For more than half of the units, both with changing or stable responses, 80% or more of the disk stimulus was contained within the receptive field center, suggesting that the stimulus had little influence on the periphery. The cell shown in Fig. 8c, for example, was an OFF ganglion cell which acquired a delayed ON response to the white disk at ND7, and additionally to the black disk at ND6. The disk stimulus was 100% contained within the receptive field center. There, stimulation of the receptive field center alone elicited luminance-dependent response changes. In this and similar cases, luminance-induced reorganization of the center-surround receptive field structure cannot account for changing response patterns.

Nevertheless, the receptive field periphery did influence the responses of many units: the responses to the local disk and full-field stimuli differed from each other at least at one light level in 67 of the 107 units. Distinct responses to localized and full-field stimulation could be observed at all light levels, from ND8 (scotopic) to ND4 (photopic), suggesting that at least some ganglion cells possess a receptive field surround in scotopic conditions.

Interestingly, we observed several units that stably maintained their response type to disks with changing luminance, but that qualitatively changed their responses to full-field steps (Fig. 8d). In these units, it is likely that a reorganization of the overall receptive field structure (e.g. of center-surround interactions) is responsible for the changes of the responses, and not a reorganization of the central receptive field alone.

Taken together, our results suggest that most units can change their responses to local stimulation, but that a dynamic reorganization of the overall receptive field structure can be responsible for some qualitative luminance-dependent response changes as well.

GABAergic inhibition involved in some response changes

GABA-mediated inhibition can mask responses of ganglion cells^{20, 21}; release from GABAergic inhibition at some light levels might therefore be a valid mechanism for luminance-dependent response changes. To test this, we compared the responses of ganglion

cells to full-field contrast steps at ND7 and ND6 with and without blockade of ionotropic GABA receptors (5 μ M SR-95531 and 100 μ M Picrotoxin, Supplementary Fig. 3a). From two retinas, we extracted 37 units with stable responses during the two repeats of ND7 in control conditions.

The drugs had diverse effects on the ganglion cell responses (for details see Supplementary Fig. 3b–e): in some cells, GABA blockers prevented luminance-dependent response changes, whereas in other cells they enabled such changes. In yet other cells responses were not influenced by GABA blockade. In summary, we found that the mechanism of GABAergic response regulation is highly diverse, and that it influences some but not all luminance-dependent qualitative response changes.

Response changes do not require rod-cone interactions

Many ganglion cells changed their response pattern at transitions within the scotopic regime (ND8/7). This suggests that rod-cone circuit interactions are not required for all response changes. To further explore how much of the response variability is brought about by the rod pathways, we used three different mouse models with non-functional cone photoreceptors (“rod-only retinas”), specifically *Gnat2^{cpfl3}*, *Cpfl1* and *Cnga3^{-/-}* mice, which carry mutations in cone-specific members of the phototransduction cascade: transducin, phosphodiesterase, and cyclic nucleotide gated channel, respectively.

In retinas from all three cone-deficient mouse lines we found a similar prevalence of luminance-dependent response changes as in wild-type retinas (Supplementary Fig. 4). Together, these results confirmed that not all luminance-dependent response changes rely on rod-cone interactions, as such changes can be observed in retinas with non-functional cones. Instead, some response changes might reflect more subtle changes in processing due to engaging different rod-mediated pathways¹¹ at low and high scotopic light levels.

Generalization to other species

To exclude that luminance-dependent response changes are a feature restricted to the mouse retina, we recorded from the isolated pig retina, using the same paradigm as for the mouse retina.

Luminance-dependent response changes were also commonly observed in pig ganglion cells (n=98 cells, three retinal pieces from two different animals, summarized in Supplementary Fig. 5). While the pig and mouse data certainly differ in some details (e.g. hardly any delayed ON responses in pig OFF cells), the phenomenon of luminance-dependent qualitative response changes was observed in both species with comparable frequency.

Discussion

We have studied the responses of retinal ganglion cells to full-field contrast steps over 5 log units of background light intensities. We classified ganglion cells into ON and OFF groups based on their linear filter and found that most OFF ganglion cells and a large fraction of ON cells behave as ON-OFF at least at some luminance levels. In both groups, the responses to the anti-preferred stimulus contrast could have short latency (early responses) or long

latency (delayed responses). Early and delayed responses, which may occur together in many cells (Fig. 3a,c), appeared to be distinct response categories (Fig. 2b) that can be regulated independently (Supplementary Fig. 3). Most intriguingly, the vast majority of cells (> 80%) displayed different response types to the anti-preferred contrast at different background luminance (Fig. 3b,d). It is noteworthy that the linear filter polarity, obtained as spike-triggered average to full-field Gaussian white noise flicker, was stable at all light intensities despite changing responses to step-stimuli.

Despite such a high degree of variability in the responses of ganglion cells, we found them to be reliably bound to the specific luminance: most cells would always respond in a similar way at a particular light level, even if such trials were interleaved with exposure to higher or lower light levels (Fig. 5). Moreover, luminance-dependent qualitative changes of the responses were also demonstrated in recordings from dLGN neurons *in-vivo* (Fig. 7) and to spatially heterogeneous stimuli, such as small disks (Fig. 8) and a naturalistic movie (Supplementary Fig. 2), which is a more ecologically relevant visual stimulus for the retina and the visual system in general. In several single-cell recordings from ganglion cells identified to be morphologically ON or OFF, similar light-dependent response changes were observed (Fig. 6), further corroborating the conclusions drawn from the MEA recordings. Finally, we found that luminance-dependent response changes are not restricted to the mouse retina, but exist in pig retina as well (Supplementary Fig. 5).

In the isolated retina, stimulation at light levels higher than ND4 (corresponding to 10^4 $R^*rod^{-1}s^{-1}$) lead to subtle changes in response properties that are likely associated with excessive bleaching of photopigment (not shown). While the retina continued to respond well to visual stimulation, the results obtained at those high intensities probably do not reflect normal retinal processing as it would happen in the intact eye (unpublished data), hence we excluded these higher light levels from our analysis. The recordings from the dLGN do therefore not only confirm that luminance-dependent response variability occurs *in-vivo*, but they also expand the range of light intensities at which that phenomenon was observed. Overall, we found luminance-dependent response changes over all intensity ranges and at each luminance transition we tested, from scotopic to photopic light levels.

The collective activity (firing pattern) of all retinal ganglion cells in response to a visual stimulus is sometimes referred to as the retinal code, which is, simply put, “what the eye tells the brain” about the stimulus²². Common research questions related to the retinal code often revolve around two topics: First, how does the retina encode the visual stimulus? Second, how might the visual brain decode the action potential pattern generated by the retinal ganglion cells? Our results have intriguing implications for both of these questions.

The first topic, encoding of visual stimuli, boils down to a mechanistic understanding of retinal circuits: How do cellular and circuit properties combine to produce certain ganglion cell responses? Decades of research have revealed fundamental aspects of this issue, ranging from the workings of the phototransduction cascade²³, to the identity of retinal cell types²⁴, to complex receptive and projective field organizations^{2, 25-27}, to adaptation to first and higher order statistics of the visual stimulus²⁸⁻³⁰. Our results suggest that it may be worth to revisit many of these functional findings and compare them in detail at different light levels.

Recent reports about the “connectome” of the inner retina can form a framework for understanding the mechanisms for the response variability we describe here. 3-dimensional electron-microscopy reconstruction of the inner mouse³¹ and rabbit³² retina showed that many bipolar cell types connect to many different ganglion cell types, including ON bipolar cells to OFF ganglion cells and vice versa. Such promiscuous connectivity was confirmed by physiological recordings in salamander retina²⁵. Additionally, some ganglion cells receive excitatory drive during anti-preferred contrast steps through gap-junction coupling with amacrine cells²⁰. These diverse connectivity patterns, in combination with amacrine cell-mediated feedback inhibition to veto synaptic release from bipolar cell terminals^{21, 25, 33}, provide all necessary building blocks for turning on or off certain inputs to ganglion cells under different (luminance) conditions. However, we have shown that the particular mechanism underlying luminance-dependent response variability may differ in different ganglion cell types. For example, two ganglion cells might change their responses during the same luminance transition for different reasons: while one cell gains a surround, the other cell remodels its central receptive field (Fig. 8). While one cell’s response variability is regulated by GABAergic inhibition, the other cell changes its responses independently of GABA (Supplementary Fig. 3). Furthermore, we found many cells to change their responses at several luminance transitions, so that even a single ganglion cell might employ diverse mechanisms at different luminance transitions. This variety of observed effects suggests that the detailed mechanisms underlying luminance-dependent response changes likely need to be investigated on the level of individual ganglion cells and their circuits.

Related to the topic of ‘encoding’ is the problem of functional classification of ganglion cell types. This question has been approached by describing ganglion cell responses with several parameters such as polarity, latency, transiency, direction selectivity etc., usually in response to simple stimuli such as full field flashes and moving bars³⁴⁻³⁶. However, as we show here, response properties of ganglion cells depend on the ambient luminance, including properties which serve as parameters used for cell classification. For example, a cell identified as an OFF cell at one luminance might behave as an ON-OFF cell at another luminance – even within the same coarse brightness range (scotopic, mesopic and photopic). Thus, two cells of the same cell type might be artificially separated into different groups if measurements were done under different luminance conditions. Consequently, using controlled and comparable luminance conditions as well as similar stimuli is crucial not only for proper comparison of response patterns between research groups, but also between several experiments within a single study. In the future, it will be important to rigorously test whether all ganglion cells of the same (morphological) type change their responses coherently during luminance transitions.

The recent advances in retinal prosthetic technology, including electrical retinal implants³⁷⁻³⁹ and optogenetic approaches⁴⁰⁻⁴³, have raised the bar on the stated goals in vision restoration: the goal is not anymore to simply confer light perception to the blind patient, but to try and fully restore the normal function. Ideally, an implant would encode the light stimulus such that the induced retinal output would be as natural as possible. Our work suggests that the “natural” retinal output is a moving target. This may, in fact, be advantageous for prosthetics that lack cellular specificity, such as electrical retinal implants.

They have always suffered from the problem of not being able to specifically stimulate ON or OFF cells (but see Cai et al⁴⁴). According to our results, ON responses are a common feature in OFF cells. Non-specific electrical stimulation at light onset might therefore not confuse the brain as much as it has been feared. Whether or not this really is the case, however, depends on how the retinal output is decoded.

The second topic, decoding of the retinal output, views the retina as a black box, and asks questions about how the output of the retina is treated by receiving neurons: Is the exact spike timing important^{45, 46}, or is the firing rate the relevant unit^{47, 48}? How is the correlation structure of multineuron firing patterns taken into account⁴⁹? When we started this research project, we expected to see a rather moderate influence of illuminance on the retinal output, maybe with more pronounced effects at certain brightness thresholds (namely cone activation threshold and rod saturation threshold). Overall, however, we assumed that adaptation in the retina largely compensates for illuminance differences, so that the “black box” delivers a rather stable input to the visual brain. Since this does not seem to be the case, there is a whole new dimension that is added to the already existing questions on decoding: How does the brain deal with the changes of the retinal output? Are they successfully filtered out and discarded, or do they indeed carry important information, maybe even used to identify current viewing conditions?

The data we presented is probably insufficient to even start tackling these questions. Furthermore, in the current work we have only focused on qualitative response changes. In addition, there are widespread quantitative changes in response to both preferred and anti-preferred contrast steps (e.g. response amplitude, transiency), as can be seen in many of the example responses depicted in our figures. Various aspects of quantitative luminance-induced changes have also been described by others^{5, 7}. In the future, it will be desirable to monitor the luminance-dependent changes of the retinal output on a better spatial scale. In particular, it will be important to test if the information transmitted to the brain by a population of ganglion cells is luminance-independent, despite the luminance-dependent changes of single cells. It is also possible that the phenomenon of “changing output”, described in this paper, allows the retina to encode the visual stimulus more efficiently in the ever-changing and dynamic luminance conditions during natural viewing¹⁵.

Methods

Animals

As wild type animals, we used PV-Cre × Thy-S-Y mice¹⁷ (B6;129P2-Pvalb<tm1(cre)Arbr>/J × C57BL/6-TG(ThystopYFPJS), and C57Bl/6J mice. For cone-deficient mice, we used *Cnga3*^{-/-} (Ref 51, kindly provided by M. Biel), *Cpfl1* mice (B6.CXB1-Pde6c<cpfl1>, Jackson strain #3678), kindly provided by Bo Chang (The Jackson Laboratory, Bar Harbor, ME), and *Gnat2*^{cpfl3} mice (B6.Cg-Gnat2<cpfl3>/Boc, Jackson strain #6795). Wild type animals were 5 weeks to 6 months at the time of the experiments, *Cnga3*^{-/-} animals were 4.5–6 weeks, *Cpfl1* animals 11–13 weeks old, and *Gnat2*^{cpfl3} animals were 12 months old. We used both, male and female mice, for all experimental paradigms. Mice were kept in groups of 1 to 5 animals. Animal use was in

accordance with German, UK and European regulations and approved by the Regierungspräsidium Tübingen (*in-vitro* experiments).

Pig retinas were obtained from two female domestic pigs sacrificed during independent scientific studies at the Department of Experimental Surgery, University Tübingen. Pigs were sedated and anesthetized by injection of Atropine, Azaperone, Benzodiazepine (Midazolam), and Ketamine, and sacrificed by Embutramide (T61). Before administration of Embutramide, Heparin was injected. During sedation and anesthesia, the pigs were dark adapted for 15–20 minutes. After death, the eyes were enucleated immediately under dim red light conditions, the cornea, lens, and vitreous removed, and the eyecup was kept in CO₂-independent culture medium (Gibco) and protected from light. After transportation to the lab, pieces of 4×4 mm² were cut from the mid-peripheral retina. Recordings were performed identically to experiments with mouse retina.

In-vitro MEA recordings

Mice were kept on a 12/12 hour light/dark cycle, dark-adapted for 4–16h before the experiment, and sacrificed under dim red light by cervical dislocation. The eyecups were removed, put in Ringer solution (in mM: 110 NaCl, 2.5 KCl, 1 CaCl₂, 1.6 MgCl₂, 10 D-Glucose, and 22 NaHCO₃) bubbled with 5% CO₂ / 95% O₂. The retina was isolated and attached to a nitrocellulose filter (Millipore) with a central 2×2 mm hole, with the optic nerve head centered. Experiments were performed at different circadian times with no noticeable effects on the outcome.

All recordings were performed with a perforated 60-electrode MEA (60pMEA200/30iR-Tigr, Multichannel Systems, Reutlingen) with square grid arrangement and 200 μm electrode distance. The mounted retina was placed ganglion cell-side down in the recording chamber, and good electrode contact was achieved by negative pressure through the perforated MEA. The tissue was superfused with Ringer solution at 34°C. Data was recorded at 25 kHz with a USB-MEA-system (USB-MEA1060, Multichannel Systems) or a MC-Card based MEA-system (MEA1060, Multichannel Systems). The detailed experimental procedure has been published before⁵¹.

Pharmacology

To block ionotropic GABA receptors, 5 μM SR-95531 (Gabazine, antagonist of GABA_A receptors, Sigma) and 100 μM Picrotoxin (antagonist of GABA_A and GABA_C receptors, Sigma) were added to the Ringer solution. SR-95531 was dissolved in water at a concentration of 5 mM; Picrotoxin was dissolved in DMSO at a concentration of 100 mM. Wash-in was performed during 10 min at a speed of approx. 1 ml/min.

Single-cell recordings, immune-staining, and confocal microscopy

Retina preparation was carried out in Ringer solution, as described for MEA recordings. The isolated retina mounted on the nitrocellulose filter was attached in the recording chamber by vacuum grease. The same setup, including visual stimulation hard- and software, was used as for the MEA recordings. Patch electrodes pulled from borosilicate glass capillaries (Science Products, GB150F-8P) were filled with an internal solution (in mM: 115 K-

gluconate, 2 KCl, 0.5 CaCl₂, 1 MgCl₂, 1.5 EGTA, 10 Hepes, 4 ATP-Na₂, 0.5 GTP-Na₃, 7.75 Neurobiotin-Cl, <1 Alexa 568) and had resistances between 4 and 8 MΩ. Recordings were made from ganglion cells of PV-Cre × Thy-S-Y mice in loose cell-attached mode or whole-cell mode using current-clamp (0 pA). Ganglion cells were targeted by two-photon imaging (920–950 nm) or chosen randomly. At the end of the recording, cells were filled with neurobiotin-containing internal solution, retinas were immersion-fixed in 4% PFA for 10 minutes at room temperature, washed in PBS, cryo-protected in 30% sucrose, frozen (at –150°C) and thawed three times and washed again in PBS. After blocking one hour in 10% normal donkey serum (NDS), 1% bovine serum albumin (BSA), 0.5% Triton X-100, 0.02% Na-azide in PBS, retinas were incubated 4–6 days with primary antibody goat-anti-ChAT⁵² (millipore, AB144P, 1:200), diluted in 3% NDS, 1% BSA, 0.5% Triton X-100, 0.02% Na-azide in PBS. Retinas were washed in PBS and incubated overnight with secondary antibody donkey-anti-goat Cy5⁵³ (Jackson ImmunoResearch, 705-175-147, 1:200) and Streptavidin-Cy3 (Jackson ImmunoResearch, 016-160-084, 1:200–1:400) or donkey-anti-goat Alexa 555⁵⁴ (Invitrogen, A-21432, 1:200) and Streptavidin Cy5 (Rockland, S000-06, 1:200), diluted in 0.5% Triton X-100 in PBS. Retinas were washed in PBS, incubated with DAPI (2.5 µg/ml in PBS) for 20 min, washed again and mounted in Vectashield (Vector Laboratories). All steps were carried out at room temperature. Confocal image stacks of the filled ganglion cells were taken on a Zeiss LSM710, using a 40× NA1.3 oil immersion objective. XY image and Z-stack size were chosen such that they covered the complete ganglion cell including its entire dendritic arbor and encompassed the full thickness of the inner plexiform layer. Dendritic stratification depths relative to ChAT bands and DAPI-stained nuclei of inner nuclear layer and ganglion cell layer were determined on several dendritic locations of each cell using a custom-written Mathematica script.

Light stimuli during in-vitro experiments

Intensities—Light stimulation was performed with a digital light processing (DLP) projector (PG-F212X-L, Sharp) and focused onto the photoreceptors through the condenser of the microscope (Supplementary Fig. 1). The light path contained a shutter and two motorized filter wheels with a set of neutral density (ND) filters (Thorlabs NE10B-A to NE50B-A), having optical densities from 1 (“ND1”) to 5 (“ND5”). To achieve light attenuation stronger than 5 log units, we serially combined an ND5-filter in one filter wheel with another ND-filter in the second filter wheel. We refer to the filter settings as ND4 (brightest setting used, 10⁴-fold light attenuation) to ND8 (darkest setting used, 10⁸-fold light attenuation). While changing the ND filters during the experiment, we closed the shutter to prevent intermittent exposure to bright light. We usually started the experiments at ND8, and step by step increased the ambient stimulation luminance by changing the ND filters by 1 unit. Unless otherwise noted, we presented the same set of visual stimuli at each ND level during an experiment.

The stimulus projector output spanned 3 log units of light intensities (i.e. 1000-fold difference between black (‘0’) and white (‘255’) pixels). We linearized the projector output, and limited our visual stimuli to the range of ‘0’ to ‘60’, with the background set to ‘30’ (Fig. 1a). As a consequence, the brightest pixels at any given ND-filter setting were 5-fold dimmer than the background illumination at the next brighter ND-setting (Fig. 1b).

Light Intensity Measurements—We measured the spectral intensity profile (in $\mu\text{W}\cdot\text{cm}^{-2}\cdot\text{nm}^{-1}$) of our light stimuli with a calibrated USB2000+ spectrophotometer (Ocean Optics). We transformed the stimulus intensity into equivalents of photoisomerizations per rod and second, assuming dark-adapted rods⁴². Briefly, the spectrum was converted to photons $\cdot\text{cm}^{-2}\cdot\text{s}^{-1}\cdot\text{nm}^{-1}$, convolved with the normalized spectrum of rod sensitivity⁵, and multiplied with the effective collection area of rods ($0.5\ \mu\text{m}^2$)⁵⁵. The results for a stimulus intensity of ‘30’ range from $1\ \text{R}^*\cdot\text{s}^{-1}$ per rod (ND8) to $10^4\ \text{R}^*\cdot\text{s}^{-1}$ per rod (ND4), see Fig. 1b. These calculations, and recordings from mice lacking functional rods and functional cones (not shown), suggest that ND8 and ND7 correspond to scotopic conditions, ND6 weakly activates cones, ND5 is fully mesopic, and ND4 is photopic. Note that our characterization of ND7 as scotopic may partly be owed to our use of rather low-contrast stimuli. We cannot exclude that stimuli with stronger contrast might activate cones already at ND7 (see e.g. refs. 5,56).

Light stimuli—All stimuli were gray-scale images with pixel values between ‘0’ (“black”) and ‘60’ (“white”). The background was kept at ‘30’ (“gray”), and the stimuli were balanced to keep the mean intensity over time at ‘30’.

Our stimulus set for MEA recordings contained: (1) *Full-field steps* (Fig. 1a,b). ON step: stepping to an intensity of ‘50’ for 2 s from the background of ‘30’ (66% Weber contrast); OFF step: stepping to ‘10’ for 2s (−66%). (2) *Full-field Gaussian flicker*, 30 s or 1 min. Screen brightness was updated every frame (60 Hz) or every other frame (30 Hz), and drawn from a Gaussian distribution with mean ‘30’ and standard deviation ‘9’. This stimulus was used to calculate the linear filters of ganglion cells⁵⁷. (3) *Disk Stimulus*: disks (diameter: $150\ \mu\text{m}$ on the retina) were presented on a gray (‘30’) background for 2s and had the same contrast as the full-field step stimulus (‘10’ for black disks, ‘50’ for white disks). They were centered over the recording electrodes. The sequence of disk locations was chosen such that the following disk was always at least $600\ \mu\text{m}$ away from the previous disk, and at least 7 white and 7 black disks were presented at each location at each ND-level. (4) *Binary Checkerboard flicker*, 15min. The screen was divided into a 40×40 checkerboard pattern; each checker covered $60\times 60\ \mu\text{m}^2$ on the retina. The intensity of each checker was updated independently from the other checkers and randomly switched between ‘10’ and ‘50’. This stimulus was used to calculate the spatial receptive field of ganglion cells. (5) *Natural movie*, 22 s. It consisted of sequences taken from the music video ‘Rip it up’ by Bill Haley (<http://www.youtube.com/watch?v=cG6n3Z7qwVs>). The contrast of the movie was compressed so that it spanned brightness values between ‘0’ and ‘60’.

We used different combinations/subsets of these stimuli in different experiments, repeated several times at each ND filter. The complete experimental stimulus set lasted at least 20 minutes at each ND. See results for details.

Our stimulus set for single cell recordings contained: (1) *Full-field steps* (see above). (2) *Full-field Gaussian flicker* (see above). (3) *Disk Stimulus* (see above). Disks were centered over the patched cell’s soma. (4) *Annulus Stimulus*: full-field contrast step (see above) with an inner hole (diameter: $500\ \mu\text{m}$ on the retina) staying at gray (‘30’) background, centered

on the patched cell's soma. The same set of stimuli was presented at each ND from ND8 to ND4, taking a total of 35 minutes. Only one cell was recorded from each retina.

Data analysis

Spike sorting—Data was high-pass filtered (500Hz, 10th-order butterworth filter), and spike waveforms and spike times were extracted from the raw data using Matlab (The Mathworks Inc., MA, USA). Spike sorting (assignment of spikes to individual units, presumably ganglion cells) was performed semi-manually with custom written software (Matlab). Quality of each unit was individually/manually assessed by inter-spike interval and spike shape variation. Data analysis was based on the spiking responses of individual units.

Calculation of cell polarities and receptive fields—We calculated linear filters in response to full-field Gaussian flicker and to binary checkerboard flicker by summing the 500 ms stimulus history before each spike. Linear filters calculated in response to the full-field flicker were used to determine cell polarity: Latency and amplitude of the first peak of the filter were determined. If the peak was positive-deflected, the cell was categorized as an ON cell. If negative-deflected, the cell was categorized as an OFF cell. Linear filters calculated in response to the binary checkerboard flicker were used to determine the spatial receptive field: For each checker, we determined the Standard Deviation (STD) along the 500ms temporal kernel. From the resulting 40x40 matrix entries, we calculated the mean and STD, set all checkers lying below mean + 4 STD to zero, fit a 2-dimensional Gaussian, and took the 2.5-sigma ellipse as a representation for the receptive field (Fig. 8c,d).

Firing rate calculation—We estimated the instantaneous firing rate by convolving the spike train (time series of 0's and 1's) with a Gaussian with sigma = 40 ms and amplitude = 0.25 sigma^{-1} ($\approx 10 \text{ Hz}$ for sigma = 40 ms), unless otherwise noted.

Algorithm to detect and classify early and delayed responses—For the step-stimuli (full-field and disks), we applied an algorithm to automatically detect ON responses in OFF cells as well as OFF responses in ON cells and to classify them as early or delayed (see Results for definitions). Responses were rejected as unreliable for specific light levels if less than 50% of them were strongly correlated with each other (“strong correlation” was defined here as pairwise Pearson correlation coefficient of at least 0.4; 0.2 for experiments where automated classification was only taken as a suggestion and manually corrected). Then we applied an automatic algorithm to detect and classify early and delayed responses at each reliable light level. Briefly, we compared the maximal firing rates during spontaneous activity on the one hand and the relevant time windows for early (50–350ms after the stimulus) and delayed (350–1000ms) responses on the other hand. If the peak firing rate in the response windows was higher than during spontaneous activity and also more correlated from trial to trial, we categorized the response as present, regardless of its absolute amplitude (i.e. binary classification ‘absent/present’). Additional checks were implemented to distinguish these responses from “tails” of sustained responses to the preferred contrast and to distinguish a delayed response from a slowly declining early response (in both cases, we checked for “valleys”, or firing rate decreases, before the

response peak). Mostly, the specific parameters used by the algorithm were based on heuristics and we made extensive checks to confirm that the automatic classification was valid. The responses to the small disk and in *Gnat2* retinas had smaller signal-to noise ratio; for those responses we treated the result of the automated algorithm only as a suggestion and confirmed each individual response by hand. Responses during GABA blocker application had different shapes in some cells (sharp peaks, thus slightly different latency distribution). Responses obtained during these experiments were checked manually and corrected where necessary. Responses of the LGN neurons were classified by hand.

We next compared the responses across light levels. Overall, a cell was classified as “stable” if, at all light levels being compared, it always had the same response type to the black step (i.e. no response, early response, delayed response, or both early and delayed response) and always the same response type to the white step. Otherwise the unit was classified as “changing”. If a cell had unreliable responses at some light level (see above), this light level was not considered for the analysis. For example, if a cell had unreliable responses at ND6, we did not compare this cell’s responses for the ND7/6 or the ND6/5 transition, but we still compared its responses between all other light levels, e.g. between ND7 and ND5. This is the reason for the different numbers of cells for each luminance transition in the plots showing the fraction of changing and stable units (e.g. Fig. 3b,d). As a consequence, a cell may be classified as “stable” even if it had unreliable responses at one or more light levels. The fraction of “changing” cells can therefore be viewed as a conservative estimate.

Analysis of movie responses—Responses to the movie typically consisted of interleaved sequences of spike bursts (“events”) and silence. To test if the response to the movie would change across light levels, we analyzed if a cell would have an “event” during some light level(s), but not other(s). This analysis proceeded in several steps: (1) *Alignment*. We calculated the average spike rate for each light level (see above) with a sigma of 10 ms, and calculated the pairwise cross-correlation to estimate the relative temporal shift of the spike trains (spiking always gets faster at higher intensities). We then aligned the spike trains across light levels. (2) *Event detection*. (a) From the aligned spikes, we calculated the average firing rate across the whole experiment with a sigma of 30 ms. Events were preliminarily defined as periods where the spike rate exceeded the mean firing rate of the 2 seconds before movie onset + 3 STD. (b) If spike bursts occur close to each other, they are fused into 1 event because the calculated firing rate does not drop below the threshold between the bursts. We therefore identified local minima in the spike rate and split events at those minima. (c) Of the resulting events we discarded those that were shorter than 20 ms and those that had a peak firing rate smaller than 5% of the second-largest event. (3) *Response strength*. We counted the spikes in each event at each light level, and converted that count into an average spike rate (number of spikes/s per movie presentation). We refer to this as the ‘activity’ of the cell during an event and at each light level. (4) *Light levels with very low activity*. Events are inherently defined by high activity. To look for qualitative response changes across light levels, we therefore identified light levels during which there was low activity during an event. We applied 2 criteria to identify such ‘silent’ light levels: (a) Comparison across light levels within an event: the activity during a ‘silent’ light level had to be lower than 10% of the maximal activity during this event. (b) Comparison across

events within a light level: The activity during a ‘silent’ event had to be less than 10% of the mean activity across all events at that light level. For analysis we counted only such events as ‘silent’ that fulfilled both criteria (dark gray in Supplementary Fig. 2).

Statistical analysis—No statistical methods were used to predetermine sample sizes, but our sample sizes are similar to those generally employed in the field. No statistical tests were required for analysis of the presented data.

In-vivo recordings

Five adult female C57 wild type mice (6–8 weeks, housed in a 12-hour light-dark cycle with 6 animals per cage) were used for experiments between 8 am and 6 pm. Mice were anaesthetized by i.p. injection of 30% (w/v) urethane (1.5 g/kg; Sigma, UK) and placed in a stereotaxic apparatus (SR-15 M; Narishige International Ltd., UK). Additional top up doses of anesthetic (0.2 g/kg) were applied as required and body temperature maintained at 37°C with a homoeothermic blanket (Harvard Apparatus, Kent, UK).

An incision to expose the skull surface was made and a small hole (~1 mm diameter) drilled 2.5 mm posterior and 2.3 mm lateral to the bregma, targeting the dorsal LGN. The pupil, contralateral to the craniotomy, was dilated with topical 1% (w/v) atropine sulphate (Sigma) and the cornea kept moist with mineral oil. A recording probe (A4X8-5 mm-50-200-413; Neuronexus, MI, USA) consisting of 4 shanks (spaced 200 μ m), each with 8 recordings sites (spaced 50 μ m) was then positioned centrally on the exposed surface in the coronal plane, and lowered to a depth of 2.5–3.3mm using a fluid filled micromanipulator (MO-10; Narishige).

Once the recording probe was in position and light responses confirmed, mice were dark adapted for 1 hour, which also allowed neuronal activity to stabilize after probe insertion. Neural signals were acquired using a Recorder64 system (Plexon, TX, USA). Signals were amplified $\times 3000$, highpass filtered at 300 Hz and digitized at 40 kHz. Multiunit activity (spikes with amplitudes $> 50\mu$ V) were saved as time-stamped waveforms and analyzed offline (see below).

Light stimuli (λ_{max} : 460nm; half peak width: ± 10 nm) were generated by a custom built LED based light source (Cairn Research Ltd.), passed through a filter wheel with various ND filters and focused onto a 5 mm diameter piece of opal diffusing glass (Edmund Optics Inc., York, UK) positioned 3 mm from the eye contralateral to the recording probe. LED intensity and filter wheel position were controlled by a PC running LabView 8.6 (National Instruments). At each intensity, starting from the lowest ($6.1 \times 10^{-01} \text{ R}^* \text{ rod}^{-1} \text{ s}^{-1}$), a 2 s light increment from background (+66% contrast) was followed by a 5 s inter-stimulus interval of background light after which a 2 s light decrement (–66% contrast) was presented. This was repeated 120 times at each background level before being increased by a factor of ten, spanning a 6 log unit range in total. Mice were otherwise kept in complete darkness.

At the end of the experiment mice were transcardially perfused with 0.1M PBS followed by 4% PFA. The brain was removed, post-fixed overnight, cryoprotected with 30% sucrose and sectioned at 50 μ m on a freezing sledge microtome. Sections were mounted with DPX

(Sigma), coverslipped, and electrode placement in the dLGN was confirmed by visualization of a fluorescence dye (Cell Tracker CM-DiI; Invitrogen Ltd. Paisley, UK) applied to the probe prior to recording.

Multichannel, multiunit recordings were analyzed in Offline Sorter (Plexon). Following removal of cross-channel artifacts, principal component based sorting was used to discriminate single units, identifiable as a distinct cluster of spikes in principal component space with a clear refractory period in their inter-spike interval distribution. Following spike sorting, data was exported to Neuroexplorer (Nex technologies, MA, USA) and MATLAB R2013a for construction of peristimulus histograms and further analysis. Light responsive units were identified as those where the peristimulus average showed a clear peak (or trough) that exceeded the 99% confidence limits estimated from a Poisson distribution derived from the prestimulus spike counts.

Corneal irradiance was measured using a calibrated spectroradiometer (Bentham Instruments, Reading, UK; Ocean Optics, FL, USA). Retinal irradiance was calculated by multiplying these values by pupil area/retinal area, based on calculations by Lyubarsky et al.⁵⁸ where pupil size of 3.2mm² and retinal area of 17.8mm² are used to generate a correction factor of 0.18. Effective photon flux was calculated by multiplying retinal irradiance by spectral transmission through the mouse lens⁵⁹. Photoisomerizations were calculated as described for MEA recordings. All procedures conformed to requirements of the UK Animals (Scientific Procedures) Act, 1986.

Supplementary Material

Refer to Web version on PubMed Central for supplementary material.

Acknowledgements

We thank Jonathan Wynne for technical assistance and M. Biel for supplying *Cnga3*^{-/-} mice. This research was supported by funds of the Deutsche Forschungsgemeinschaft (DFG) to the Werner Reichardt Centre for Integrative Neuroscience (DFG EXC 307), by the Bundesministerium für Bildung und Forschung (BMBF) to the Bernstein Center for Computational Neuroscience (FKZ 01GQ1002), by funds of the Biotechnology and Biological Sciences Research Council (BBSRC BB/1007296/1) and the European Commission (ERC Advanced Grant MeloVision) to R.J.L., a Christiane-Nüsslein-Volhard Stipend to A.T.H, and a Pro-Retina Stipend to K.R.

References

1. O'Brien BJ, Isayama T, Richardson R, Berson DM. Intrinsic physiological properties of cat retinal ganglion cells. *J Physiol.* 2002; 538:787–802. [PubMed: 11826165]
2. Gollisch T, Meister M. Eye smarter than scientists believed: neural computations in circuits of the retina. *Neuron.* 2010; 65:150–164. [PubMed: 20152123]
3. Reitner A, Sharpe LT, Zrenner E. Is colour vision possible with only rods and blue-sensitive cones? *Nature.* 1991; 352:798–800. [PubMed: 1881435]
4. Enroth-Cugell C, Lennie P. The control of retinal ganglion cell discharge by receptive field surrounds. *J Physiol.* 1975; 247:551–578. [PubMed: 1142301]
5. Farrow K, et al. Ambient illumination toggles a neuronal circuit switch in the retina and visual perception at cone threshold. *Neuron.* 2013; 78:325–338. [PubMed: 23541902]
6. Sagdullaev BT, McCall MA. Stimulus size and intensity alter fundamental receptive-field properties of mouse retinal ganglion cells in vivo. *Vis Neurosci.* 2005; 22:649–659. [PubMed: 16332276]

7. Grimes WN, Schwartz GW, Rieke F. The synaptic and circuit mechanisms underlying a change in spatial encoding in the retina. *Neuron*. 2014; 82:460–473. [PubMed: 24742466]
8. Umino Y, Solessio E, Barlow RB. Speed, spatial, and temporal tuning of rod and cone vision in mouse. *J Neurosci*. 2008; 28:189–198. [PubMed: 18171936]
9. Protti DA, Flores-Herr N, Li W, Massey SC, Wassle H. Light signaling in scotopic conditions in the rabbit, mouse and rat retina: a physiological and anatomical study. *J Neurophysiol*. 2005; 93:3479–3488. [PubMed: 15601738]
10. Eggers ED, Mazade RE, Klein JS. Inhibition to retinal rod bipolar cells is regulated by light levels. *J Neurophysiol*. 2013; 110:153–161. [PubMed: 23596335]
11. Bloomfield SA, Dacheux RF. Rod vision: pathways and processing in the mammalian retina. *Prog Retin Eye Res*. 2001; 20:351–384. [PubMed: 11286897]
12. Ke JB, et al. Adaptation to background light enables contrast coding at rod bipolar cell synapses. *Neuron*. 2014; 81:388–401. [PubMed: 24373883]
13. Dunn FA, Doan T, Sampath AP, Rieke F. Controlling the gain of rod-mediated signals in the Mammalian retina. *J Neurosci*. 2006; 26:3959–3970. [PubMed: 16611812]
14. Dunn FA, Lankheet MJ, Rieke F. Light adaptation in cone vision involves switching between receptor and post-receptor sites. *Nature*. 2007; 449:603–606. [PubMed: 17851533]
15. Allen AE, et al. Melanopsin-Driven Light Adaptation in Mouse Vision. *Curr Biol*. 2014
16. Manookin MB, Beaudoin DL, Ernst ZR, Flagel LJ, Demb JB. Disinhibition combines with excitation to extend the operating range of the OFF visual pathway in daylight. *J Neurosci*. 2008; 28:4136–4150. [PubMed: 18417693]
17. Munch TA, et al. Approach sensitivity in the retina processed by a multifunctional neural circuit. *Nat Neurosci*. 2009; 12:1308–1316. [PubMed: 19734895]
18. Pitkow X, Meister M. Decorrelation and efficient coding by retinal ganglion cells. *Nat Neurosci*. 2012; 15:628–635. [PubMed: 22406548]
19. Kuffler SW. Discharge patterns and functional organization of mammalian retina. *J Neurophysiol*. 1953; 16:37–68. [PubMed: 13035466]
20. Farajian R, Pan F, Akopian A, Volgyi B, Bloomfield SA. Masked excitatory crosstalk between the ON and OFF visual pathways in the mammalian retina. *J Physiol*. 2011; 589:4473–4489. [PubMed: 21768265]
21. Roska B, Werblin F. Vertical interactions across ten parallel, stacked representations in the mammalian retina. *Nature*. 2001; 410:583–587. [PubMed: 11279496]
22. Meister M, Berry MJ 2nd. The neural code of the retina. *Neuron*. 1999; 22:435–450. [PubMed: 10197525]
23. Lamb TD, Pugh EN Jr. Phototransduction, dark adaptation, and rhodopsin regeneration the proctor lecture. *Invest Ophthalmol Vis Sci*. 2006; 47:5137–5152. [PubMed: 17122096]
24. Werblin FS, Dowling JE. Organization of the retina of the mudpuppy, *Necturus maculosus*. II. Intracellular recording. *J Neurophysiol*. 1969; 32:339–355. [PubMed: 4306897]
25. Asari H, Meister M. The projective field of retinal bipolar cells and its modulation by visual context. *Neuron*. 2014; 81:641–652. [PubMed: 24507195]
26. Lukasiewicz PD. Synaptic mechanisms that shape visual signaling at the inner retina. *Prog Brain Res*. 2005; 147:205–218. [PubMed: 15581708]
27. Thoreson WB, Mangel SC. Lateral interactions in the outer retina. *Prog Retin Eye Res*. 2012; 31:407–441. [PubMed: 22580106]
28. Baccus SA, Meister M. Fast and slow contrast adaptation in retinal circuitry. *Neuron*. 2002; 36:909–919. [PubMed: 12467594]
29. Smirnakis SM, Berry MJ, Warland DK, Bialek W, Meister M. Adaptation of retinal processing to image contrast and spatial scale. *Nature*. 1997; 386:69–73. [PubMed: 9052781]
30. Tkacik G, Ghosh A, Schneidman E, Segev R. Adaptation to changes in higher-order stimulus statistics in the salamander retina. *PLoS One*. 2014; 9:e85841. [PubMed: 24465742]
31. Helmstaedter M, et al. Connectomic reconstruction of the inner plexiform layer in the mouse retina. *Nature*. 2013; 500:168–174. [PubMed: 23925239]

32. Lauritzen JS, et al. ON cone bipolar cell axonal synapses in the OFF inner plexiform layer of the rabbit retina. *J Comp Neurol.* 2013; 521:977–1000. [PubMed: 23042441]
33. Geffen MN, de Vries SE, Meister M. Retinal ganglion cells can rapidly change polarity from Off to On. *PLoS Biol.* 2007; 5:e65. [PubMed: 17341132]
34. Farrow K, Masland RH. Physiological clustering of visual channels in the mouse retina. *J Neurophysiol.* 2011; 105:1516–1530. [PubMed: 21273316]
35. Rockhill RL, Daly FJ, MacNeil MA, Brown SP, Masland RH. The diversity of ganglion cells in a mammalian retina. *J Neurosci.* 2002; 22:3831–3843. [PubMed: 11978858]
36. Zeck GM, Masland RH. Spike train signatures of retinal ganglion cell types. *Eur J Neurosci.* 2007; 26:367–380. [PubMed: 17650112]
37. Dorn JD, et al. The Detection of Motion by Blind Subjects With the Epiretinal 60-Electrode (Argus II) Retinal Prosthesis. *JAMA Ophthalmol.* 2013; 131:183–189. [PubMed: 23544203]
38. Wang L, et al. Photovoltaic retinal prosthesis: implant fabrication and performance. *J Neural Eng.* 2012; 9:046014. [PubMed: 22791690]
39. Zrenner E, et al. Subretinal electronic chips allow blind patients to read letters and combine them to words. *Proc Biol Sci.* 2011; 278:1489–1497. [PubMed: 21047851]
40. Bi A, et al. Ectopic expression of a microbial-type rhodopsin restores visual responses in mice with photoreceptor degeneration. *Neuron.* 2006; 50:23–33. [PubMed: 16600853]
41. Busskamp V, Picaud S, Sahel JA, Roska B. Optogenetic therapy for retinitis pigmentosa. *Gene therapy.* 2011; 19:169–175. [PubMed: 21993174]
42. Lagali PS, et al. Light-activated channels targeted to ON bipolar cells restore visual function in retinal degeneration. *Nat Neurosci.* 2008; 11:667–675. [PubMed: 18432197]
43. Nirenberg S, Pandarinath C. Retinal prosthetic strategy with the capacity to restore normal vision. *Proc Natl Acad Sci U S A.* 2012; 109:15012–15017. [PubMed: 22891310]
44. Cai C, Twyford P, Fried S. The response of retinal neurons to high-frequency stimulation. *J Neural Eng.* 2013; 10:036009. [PubMed: 23594620]
45. Jacobs AL, et al. Ruling out and ruling in neural codes. *Proc Natl Acad Sci U S A.* 2009; 106:5936–5941. [PubMed: 19297621]
46. Rathbun DL, Alitto HJ, Weyand TG, Usrey WM. Interspike interval analysis of retinal ganglion cell receptive fields. *J Neurophysiol.* 2007; 98:911–919. [PubMed: 17522169]
47. Berry MJ, Warland DK, Meister M. The structure and precision of retinal spike trains. *Proc Natl Acad Sci U S A.* 1997; 94:5411–5416. [PubMed: 9144251]
48. Funke K, Worgotter F. On the significance of temporally structured activity in the dorsal lateral geniculate nucleus (LGN). *Prog Neurobiol.* 1997; 53:67–119. [PubMed: 9330424]
49. Schnitzer MJ, Meister M. Multineuronal firing patterns in the signal from eye to brain. *Neuron.* 2003; 37:499–511. [PubMed: 12575956]
50. Paxinos G, FK. *The Mouse Brain in Stereotaxic Coordinates.* Academic Press; 2001.
51. Reinhard K, et al. Step-by-step instructions for retina recordings with perforated multi electrode arrays. *PLoS One.* 2014; 9:e106148. [PubMed: 25165854]
52. Yonehara K, et al. Spatially asymmetric reorganization of inhibition establishes a motion-sensitive circuit. *Nature.* 2011; 469:407–410. [PubMed: 21170022]
53. Gavrikov KE, Nilson JE, Dmitriev AV, Zucker CL, Mangel SC. Dendritic compartmentalization of chloride cotransporters underlies directional responses of starburst amacrine cells in retina. *Proc Natl Acad Sci U S A.* 2006; 103:18793–18798. [PubMed: 17124178]
54. Hoover JL, Bond CE, Hoover DB, Defoe DM. Effect of neurturin deficiency on cholinergic and catecholaminergic innervation of the murine eye. *Exp Eye Res.* 2014; 122:32–39. [PubMed: 24657391]
55. Nikonov SS, Kholodenko R, Lem J, Pugh EN Jr. Physiological features of the S- and M-cone photoreceptors of wild-type mice from single-cell recordings. *J Gen Physiol.* 2006; 127:359–374. [PubMed: 16567464]
56. Szikra T, et al. Rods in daylight act as relay cells for cone-driven horizontal cell-mediated surround inhibition. *Nat Neurosci.* Oct 26.2014

57. Chichilnisky EJ. A simple white noise analysis of neuronal light responses. *Network*. 2001; 12:199–213. [PubMed: 11405422]
58. Lyubarsky AL, Daniele LL, Pugh EN Jr. From candelas to photoisomerizations in the mouse eye by rhodopsin bleaching in situ and the light-rearing dependence of the major components of the mouse ERG. *Vision Res*. 2004; 44:3235–3251. [PubMed: 15535992]
59. Jacobs GH, Williams GA. Contributions of the mouse UV photopigment to the ERG and to vision. *Doc Ophthalmol*. 2007; 115:137–144. [PubMed: 17479214]

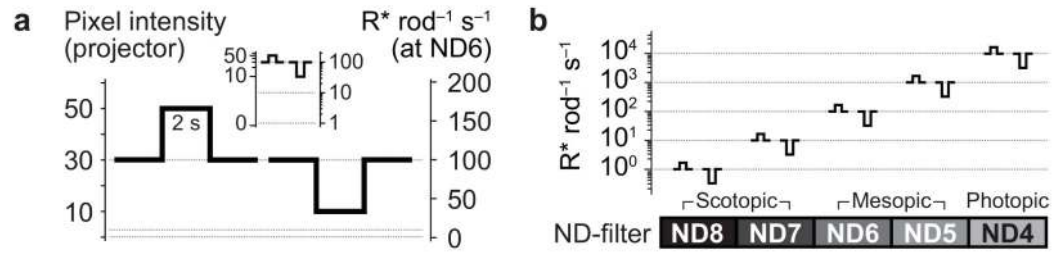


Figure 1. Overview of experimental paradigm.

(a) Light stimuli were gray scale images on a gray background. The full-field step stimulus had a Weber contrast of $\pm 66\%$. (b) Absolute intensity of stimuli, converted to $R^* \text{ rod}^{-1} \text{ s}^{-1}$, as a function of the ambient luminance set by neutral density (ND) filters.

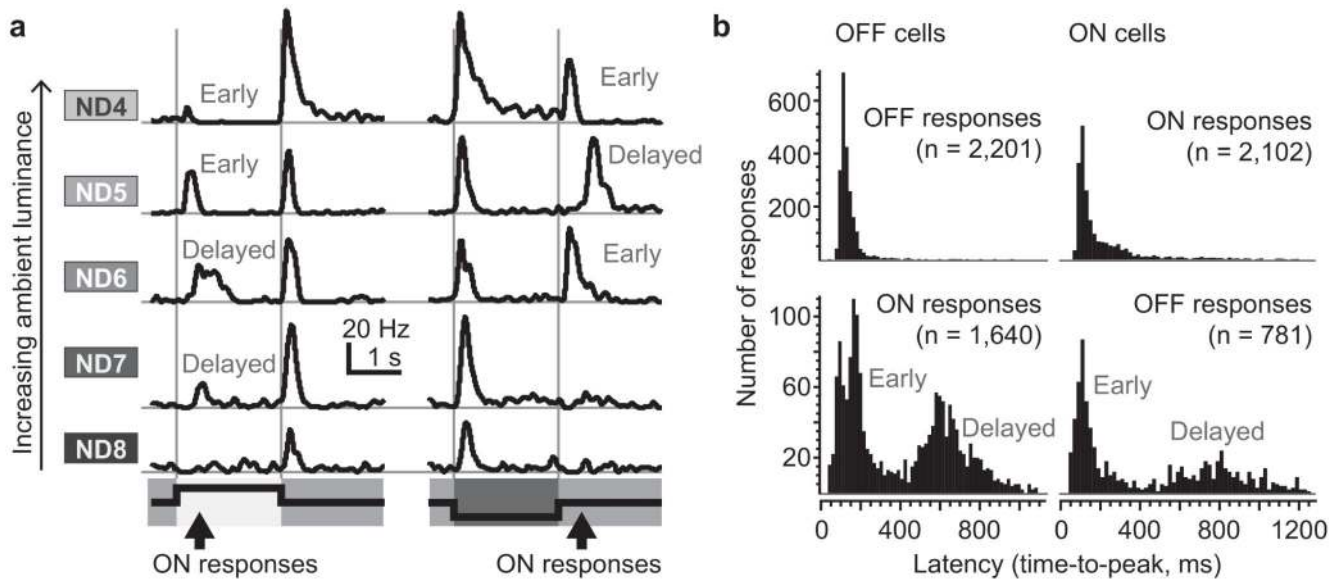


Figure 2. Early and delayed anti-preferred responses.

(a) Responses (firing rate) of a single OFF ganglion cell to white and black full-field contrast steps (average firing rate to 45 repetitions at each of five different light levels, ND8 to ND4). (b) Histogram of response latencies (time-to-peak) in OFF cells (left column) and ON cells (right column), measured from responses of all units at all light levels, to both black and white full-field steps.

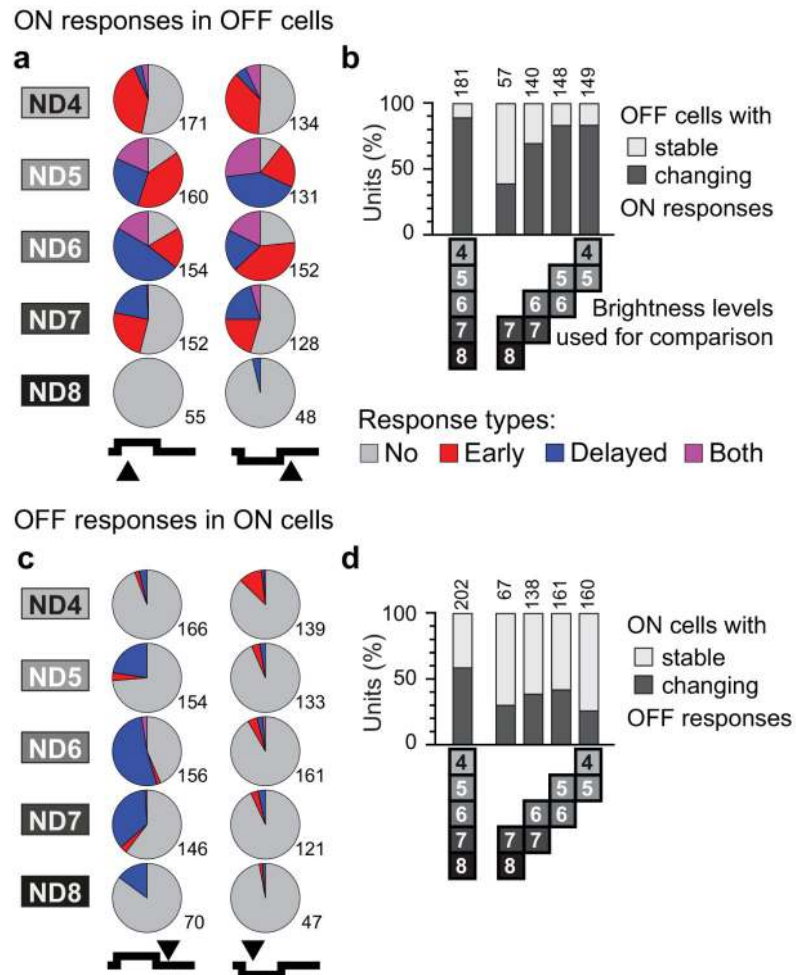


Figure 3. Summary of luminance-dependent response types.

(a) Fraction of OFF cells displaying no, early and delayed ON responses at each luminance level to white and black full-field step stimuli. (b) Fraction of units with stable and changing responses. Cells were defined as “stable” if they had the same response type (no, early, delayed, both) at all compared light levels, both to the black step and to the white step. All other cells were “changing”. (c,d) Same statistics as in a and b for OFF responses in ON cells. Numbers: Units included in the analysis due to their reliable responses at these light levels (see Methods).

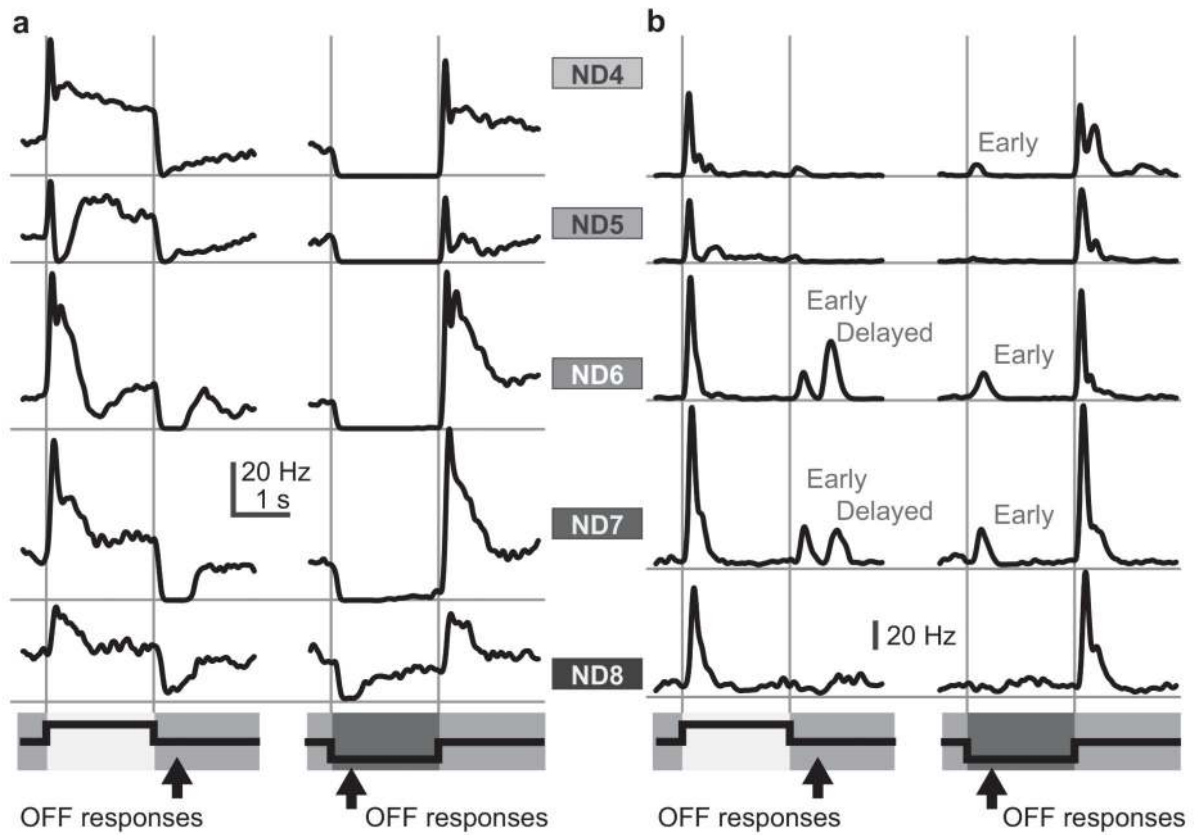


Figure 4. Responses (firing rate) of two ON ganglion cells.

Stimulus was a 2-s white or black full-field step, presented at different ambient light levels.

(a) Many ON ganglion cells were strongly suppressed by OFF stimuli. (b) ON ganglion cell with asymmetric and changing OFF responses.

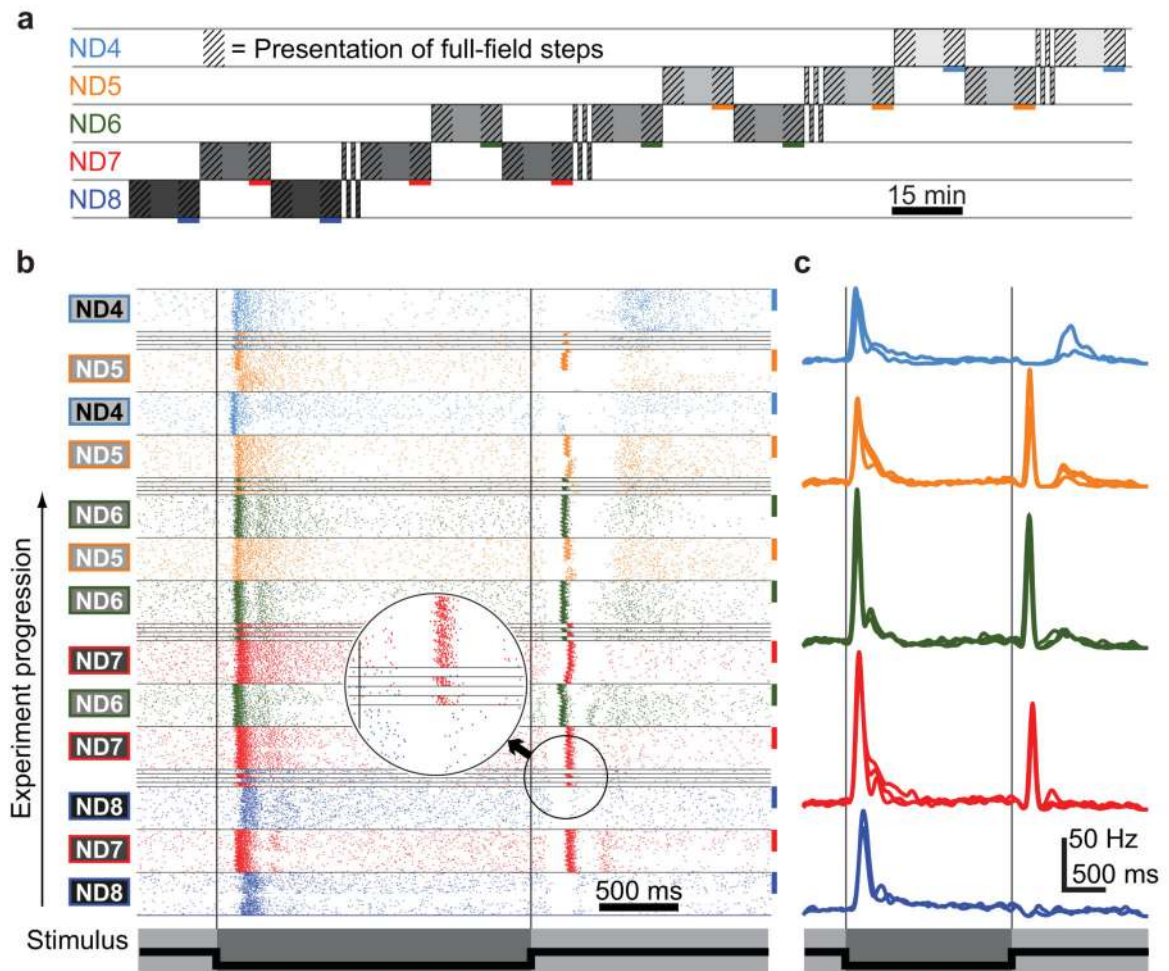


Figure 5. Stability of responses at individual light levels.

(a) Experimental protocol. Colored bars label the last 5 min at each light level. (b) Raster plot of the responses of a single unit to all 730 presentations of the black full-field step (50 repetitions during each 15 min sequence, 5 repetitions during each 1 min sequence). Even quick luminance changes are immediately reflected in a different response pattern (see magnification). Colored bars mark the same experimental sections as in a. (c) Average spike rate of the responses marked by colored bars in a and b.

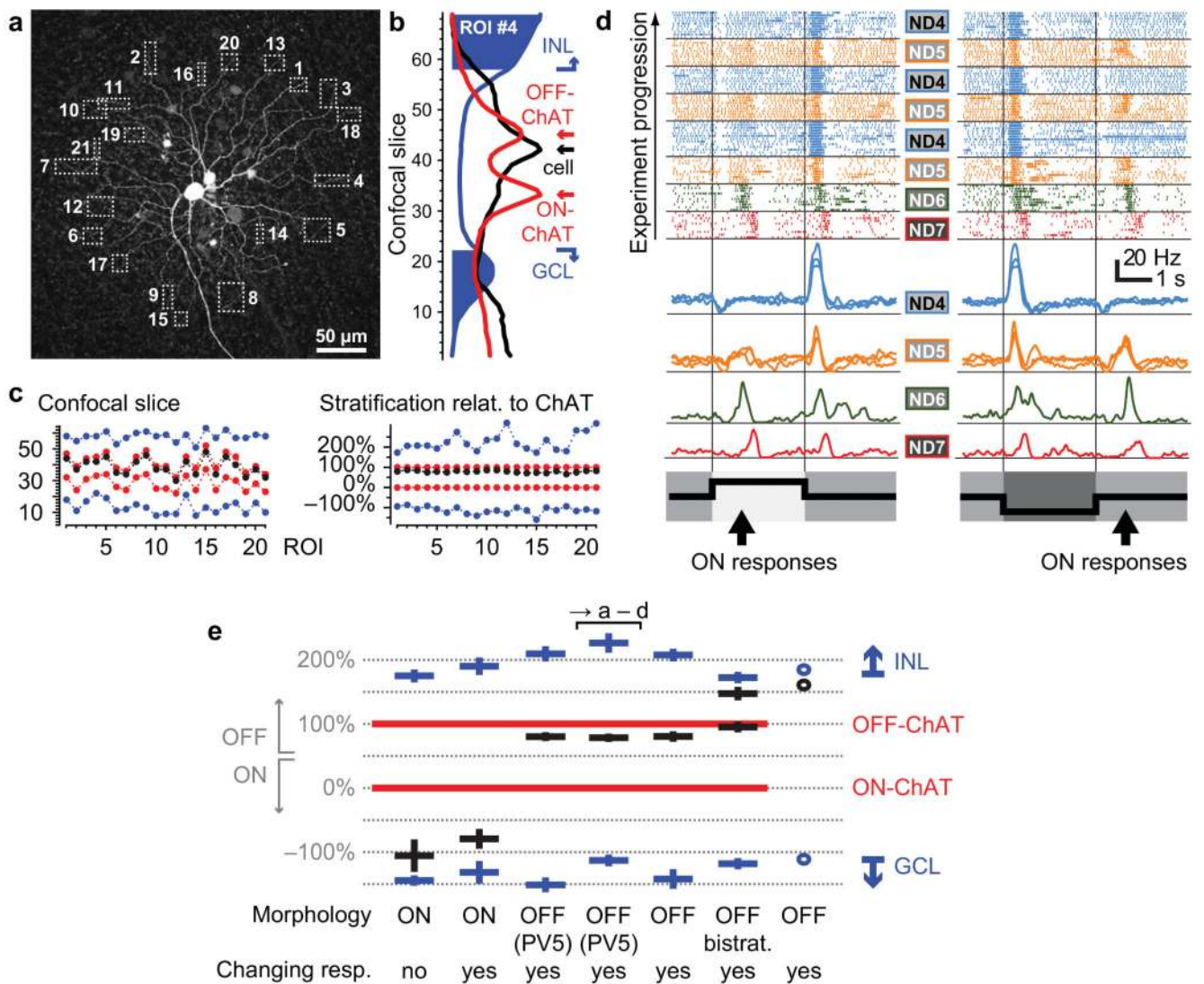


Figure 6. Responses recorded from individual ganglion cells.

(a–d) Results from one PV5 ganglion cell. (a) Maximum-intensity projection of a confocal stack, showing the neurobiotin-filled PV5 ganglion cell and the regions of interests (ROIs) used for analyzing stratification level. (b) Fluorescence intensity profile along z-axis of ROI 4. Blue: DAPI label, Red: ChAT label, Black: Neurobiotin label. Stratification levels of cell and ChAT bands: peaks of their intensity profiles. Borders of inner nuclear layer (INL) and ganglion cell layer (GCL): where the intensity profile dropped below 67% of its peak. (c) Left: Stratification measurements for each ROI, as in **b**. Right: Conversion of stratification relative to ChAT bands. (d) This OFF-stratifying cell had pronounced delayed ON responses from ND7 to ND5. (e) Dendritic stratification level (black, mean \pm s.e.m., relative to the ChAT bands, red) of individually recorded cells. For right-most cell, ChAT staining was not successful. Most cells had luminance-dependent response changes.

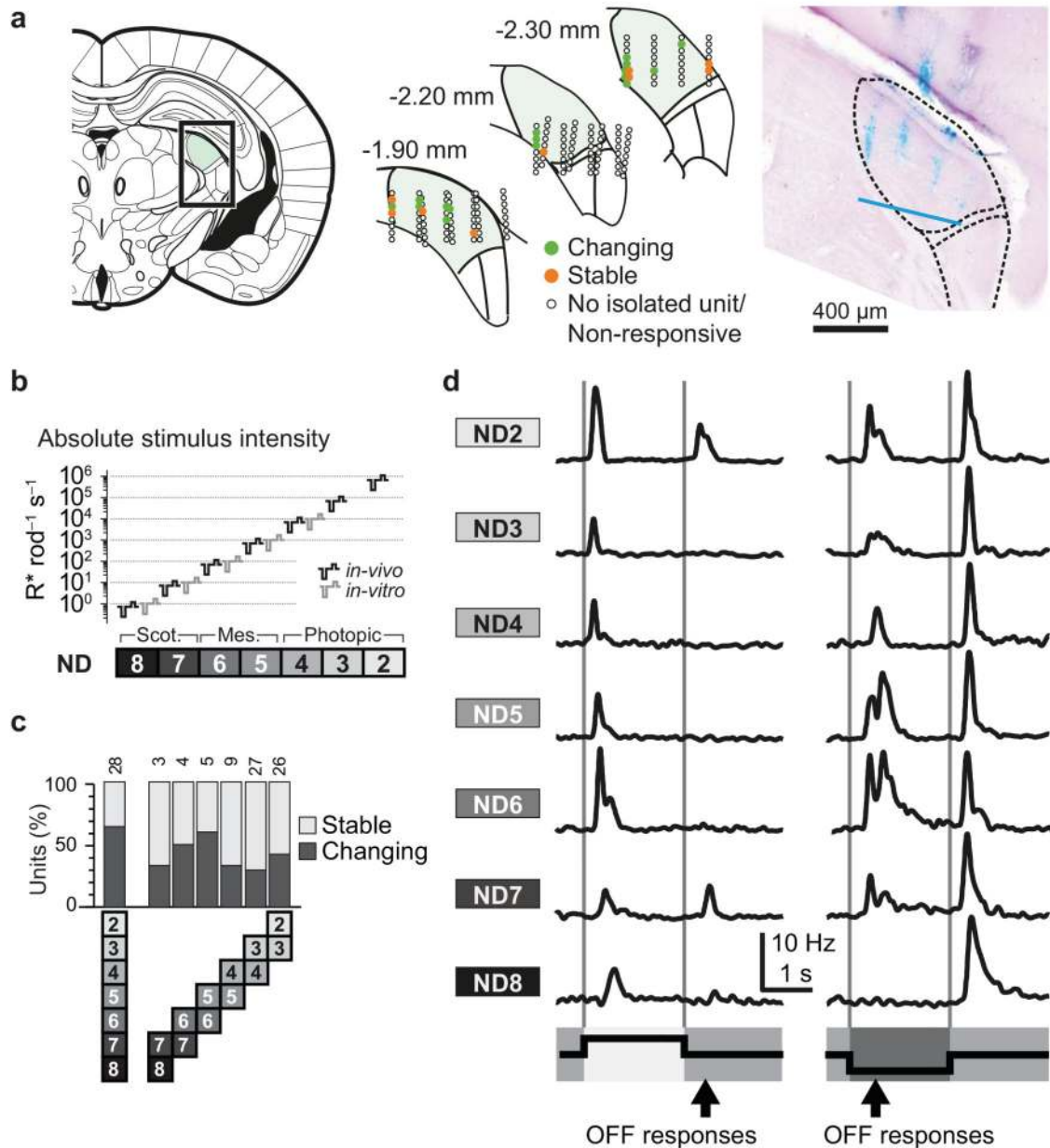


Figure 7. Luminance-dependent qualitative response changes in the dorsal lateral geniculate nucleus (dLGN).

(a) Recording locations in the dLGN, highlighted on the left). Middle: reconstructed positions (colored dots) of recording sites in three rostro-caudal positions relative to bregma. Reconstruction was based on DiI labeling of electrode shanks (right). Blue line: maximum depth of recording electrode. Brain schematics based on Paxinos et al.⁵⁰ (b) Absolute stimulus intensities used for the *in-vivo* experiments (black) in comparison to the intensities used during *in-vitro* experiments (gray, see Fig. 1b). Note that the stimulus range is extended to higher intensities. (c) Fraction of light-responsive units in the dLGN with changing or stable responses. Conventions as in Fig. 3b. (d) A single ON unit from the dLGN that has both changing and asymmetric OFF responses at different ambient light levels.

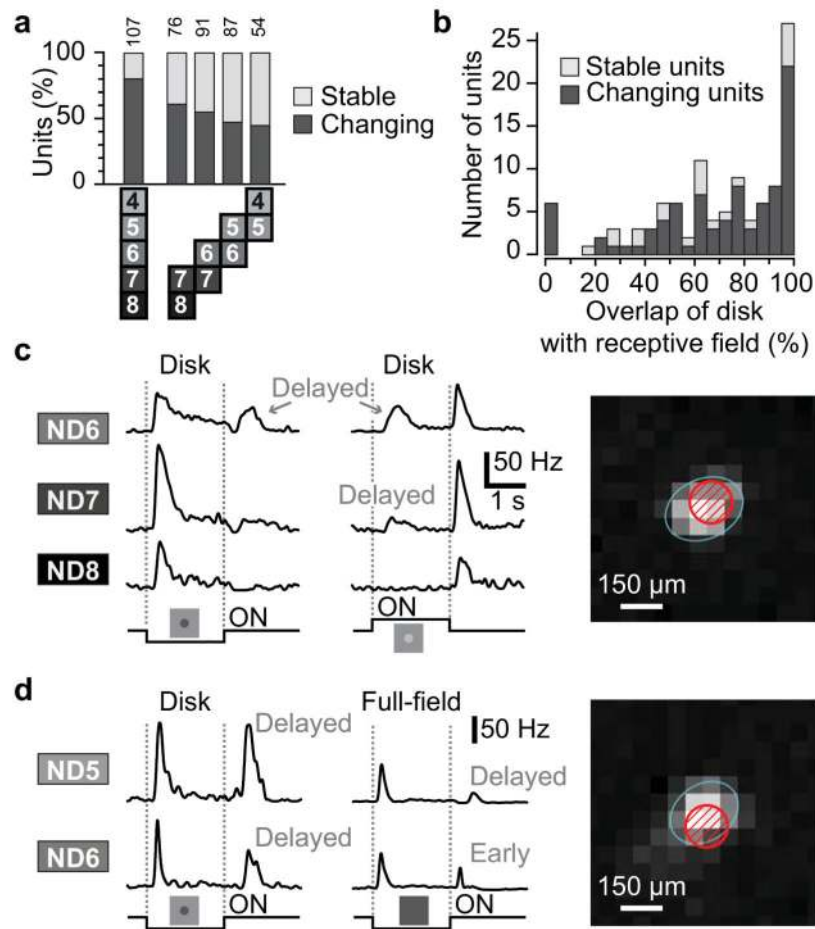


Figure 8. Luminance-dependent response changes to small localized disk stimuli.

(a) Percentage of units with stable or changing responses across different luminance levels. Conventions as in Fig. 3b, but combining both ON and OFF cells. (b) Histogram showing how much of the disk stimulus was contained within the receptive field center, as determined by a binary checkerboard flicker stimulus. (c) Example unit changing its responses to localized stimulation of the receptive field center. Right: Overlap of the disk stimulus (red) with the receptive field (blue ellipse shows 2.5-sigma of Gaussian fit). (d) Example unit that had stable responses to the disk stimulus, but changing responses to the full-field step at the ND6/5 luminance transition.